

FORMING EARLY-TYPE GALAXIES IN GROUPS PRIOR TO CLUSTER ASSEMBLY

STEFAN J. KAUTSCH,¹ ANTHONY H. GONZALEZ,¹ CHRISTIAN A. SOTO,¹ KIM-VY H. TRAN,²

DENNIS ZARITSKY,³ AND JOHN MOUSTAKAS⁴

Received 2008 July 18; accepted 2008 September 26; published 2008 October 14

ABSTRACT

We study a unique protocluster of galaxies, the supergroup SG1120–1202. We quantify the degree to which morphological transformation of cluster galaxies occurs prior to cluster assembly in order to explain the observed early-type fractions in galaxy clusters at $z = 0$. SG1120–1202 at $z \sim 0.37$ is composed of four gravitationally bound groups that are expected to coalesce into a single cluster by $z = 0$. Using *HST* ACS observations, we compare the morphological fractions of the supergroup galaxies to those found in a range of environments. We find that the morphological fractions of early-type galaxies ($\sim 60\%$) and the ratio of S0 to elliptical galaxies (0.5) in SG1120–1202 are very similar to clusters at comparable redshift, consistent with preprocessing in the group environment playing the dominant role in establishing the observed early-type fraction in galaxy clusters.

Subject headings: galaxies: clusters: general — galaxies: elliptical and lenticular, cD — galaxies: evolution — galaxies: interactions — galaxies: spiral — galaxies: structure

1. INTRODUCTION

Our understanding of the role of environment in determining galaxy properties remains incomplete primarily because of the complicated correlations among galaxy properties and the difficulty in establishing the correspondence between local galaxies and their progenitors. While many properties, including morphology and star formation rate, vary strongly as a function of environment (e.g., Dressler 1980; Lewis et al. 2002; Gómez et al. 2003) the relative importance of different physical processes in driving these variations remains controversial (Park et al. 2007). Here, we focus on identifying the environment in which predominantly late-type field galaxies are “transformed” into early-type cluster galaxies.

Two general classes of physical scenarios have been proposed as mechanisms for driving morphological transformations: local processes like mergers (e.g., Toomre 1977) or tidal interactions (e.g., Mastropietro et al. 2005) and global processes such as ram pressure stripping (e.g., Gunn & Gott 1972), evaporation and strangulation (e.g., Larson et al. 1980), and harassment (e.g., Moore et al. 1999). Local processes are most effective in groups because of the low relative velocities (Barnes 1985) whereas global processes are most effective in clusters where the gravitational potential is deep but the relative velocities of the galaxies are high.

A compelling empirical case has been made that preprocessing in the group environment is the dominant mechanism driving the observed early-type fractions in clusters (Zabludoff & Mulchaey 1998; Kodama et al. 2001; Helsdon & Ponman 2003). However, numerical simulations have recently suggested that intermediate-mass clusters accrete their galaxies as individual systems, and that therefore any transformation must occur in the cluster environment (Berrier et al. 2008). Evidently, the key in resolving this question lies in unambiguously tagging and studying the distant galaxies that lie in today’s massive clusters.

The natural environment to begin such a study is that of groups at intermediate redshift (e.g., Wilman et al. 2005; Mulchaey et al. 2006). However, not all groups will be accreted by clusters and there exists a wide dispersion in group properties at intermediate redshifts (Poggianti et al. 2006). To avoid these pitfalls, we focus on a unique system,⁵ SG1120–1202 (hereafter SG1120). SG1120 is a gravitationally bound structure consisting of four X-ray-luminous groups at $z \sim 0.37$, whose dynamics indicate that it will collapse to form a cluster of similar mass to Coma by $z = 0$ (Gonzalez et al. 2005). Therefore, the question is relatively unambiguous here: do the galaxy morphologies in SG1120 already match those seen in local clusters of comparable mass or will they need to be transformed after the groups coalesce? While SG1120 represents only one unique evolutionary path, most clusters continue to accrete groups at late times and the group properties observed in SG1120 are broadly relevant for assessing the impact of this late-type accretion. In this Letter we use the standard cosmology ($\Omega_m = 0.3$, $\Omega_\Lambda = 0.7$, $H_0 = 70 \text{ km s}^{-1} \text{ Mpc}^{-1}$) unless stated otherwise.

2. OBSERVATIONS

We measure morphologies using *HST* ACS F814W imaging (Cycle 14) composed of 10 pointings that cover $18.4' \times 11.8'$, with single-orbit depth at each location. Spectra were obtained with the VLT (VIMOS and FORS2; 2004 February and 2007 February) and Magellan (LDSS3; 2006 February) and ground-based imaging with the VLT (VIMOS; 2003 February and 2006 February) and the KPNO Mayall (FLAMINGOS; 2006 February) telescopes. The spectroscopic target selection was based on Vega-magnitude-limited catalogs ($R \leq 22.5$ or $K_s \leq 20$). The observations yield redshifts for 364 galaxies, including 156 confirmed SG1120 members on the *HST* ACS mosaic. Confirmed members are defined to lie within the 2σ velocity limits defined by the lowest and highest redshift groups (890 and 1551 km s^{-1} , respectively), which in turn corresponds to

¹ Department of Astronomy, University of Florida, Gainesville, FL 32611-2055.

² Institute for Theoretical Physics, Universität Zürich, CH-8057 Zürich, Switzerland.

³ Steward Observatory, University of Arizona, Tucson, AZ 85721.

⁴ Center for Cosmology and Particle Physics, New York University, 4 Washington Place, New York, NY 10003.

⁵ Based on observations with the NASA/ESA Hubble Space Telescope, obtained at the Space Telescope Science Institute, which is operated by AURA, Inc., under NASA contract NAS 5-26555; and based on data collected at the VLT (072.A-0367, 076.B-0362, and 078.B-0409), which is operated by ESO and the Magellan Telescope, which is operated by the Carnegie Observatories.

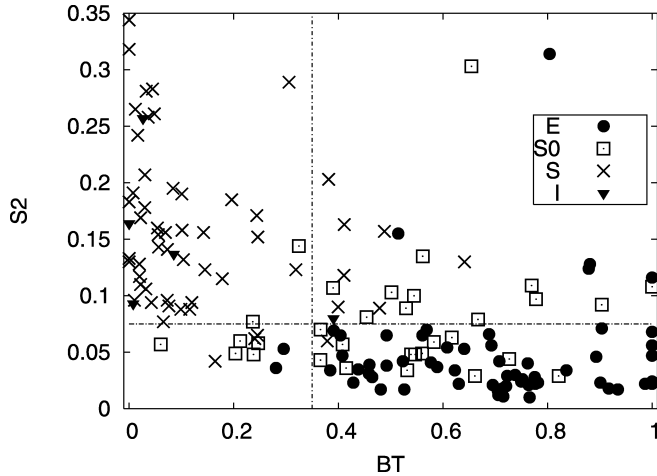


FIG. 1.—Comparison of the visual morphologies (as indicated in the legend) to the GIM2D values. The quantitative bulge-to-total ratio (BT) is plotted on the x-axis and smoothness index (S2) on the y-axis. The horizontal and vertical lines indicate the values separating our morphological classes based on the criteria by Simard et al. (2008).

$0.349 \leq z \leq 0.377$. The velocity dispersions for the groups are measured using the biweight estimator (rostat; Beers et al. 1990).

For the subsequent computation we use $M_V^* = -21.28$ ($m_{814} = 19.1$, Vega) as in Postman et al. (2005). For the photometric filter conversions including evolution correction we use the formulae from Fabricant et al. (2000) which have a 0.1 mag associated uncertainty.

3. MORPHOLOGICAL CLASSIFICATION

3.1. Quantitative Classification

We use GIM2D (Simard et al. 2002, 2008) for the quantitative morphological classification. GIM2D performs automated bulge/disk decomposition and measures the object's asymmetry. We compare our morphological results with the reference data set of Simard et al. (2008) who used the same quantitative classification on a morphological study of high-redshift galaxy clusters and groups in the ESO Distant Cluster Survey.

The galaxies are modeled using an $r^{1/4}$ profile for the bulge and an exponential profile for the disk, and the models are convolved with the point-spread function (PSF) generated by TinyTim (Krist 1993). For each object, we calculate PSFs at the locations of the members in the raw ACS images, and then drizzle (Fruchter & Hook 2002) them together to generate a composite PSF for each object.

For each galaxy, we use the GIM2D bulge-to-total ratio (BT) and image smoothness index (S2) (Simard et al. 2008) inside two half-light radii; S2 measures the overall smoothness of the galaxy with respect to the model.

3.1.1. Reliability Tests with Simulations

A reliability check of GIM2D and error quantification is performed by inserting artificial galaxies (created with GAL-IMAGE/GIM2D) in the real ACS frames that are then analyzed in the same way as the observed galaxies. We follow the description given by Simard et al. (2002, 2008). The simulated galaxies have random BT and inclination values between 0 and 1 and 0° and 85° , respectively, and cover the magnitude range of our targets. We derive the averaged standard deviation for

BT ($=0.042$) and S2 ($=0.016$) with the aid of the simulations. We then perform bootstrap resampling to compute a fractional error of 4% using the standard deviations determined the simulations. Therefore we assume an uncertainty of $\pm 4\%$ for the quantitative morphological fractions derived throughout this Letter.

3.2. Visual Classification

To complement our quantitative morphologies, five of our team members⁶ visually classified all confirmed cluster members according to a simplified Hubble scheme: ellipticals (E), lenticulars (S0), spirals (S), and irregulars (I). For this analysis the irregular classification includes interacting and low surface brightness galaxies as well as dwarfs. To standardize the classifications, we use a training set based on the sample from Fabricant et al. (2000). For the subsequent analysis, we adopt the most common assigned morphological type when the classification from the individuals differs.

3.3. Visual versus Quantitative Classification

Figure 1 shows the distribution of the visual types (E, S0, S, and I) and their GIM2D values. A correlation is evident in Figure 1, with E+S0 galaxies typically having $0.4 \leq BT \leq 1$ (right) and S galaxies $BT < 0.4$ (left). Asymmetric structures, measured with S2, increase in late-type galaxies as expected. However, the divisions are not sharp and each class contains some galaxies that lie outside these regions. Asymmetric structures such as rings, spiral arms, H II regions, and the presence of close neighbors can contribute to the scatter in BT for S0, S, and I galaxies. Moreover, the spread in BT range is not surprising given that spheroids do not all have $r^{1/4}$ profiles, and not all disks are pure exponentials (e.g., Graham et al. 2003).

Simard et al. (2008) derived the fraction of early-type galaxies, f_e , using the same GIM2D criteria as in this Letter. We use their definition for early-types as being galaxies with $BT \geq 0.35$ and $S2 \leq 0.075$ (cf. Tran et al. 2001). The values of these selection criteria are indicated by a vertical and horizontal line in Figure 1. We find that many galaxies that qualify as late-types by the quantitative criteria, but that are visually classified as S0, generally have moderate quantitative asymmetry.

4. EARLY-TYPE FRACTIONS

The early-type fraction (f_e) depends both on how f_e is defined (visual vs. GIM2D) and the magnitude limit. The visual and quantitative morphologies yield nearly identical fractions. We derive f_e for different magnitude limits and list the results for SG1120 in Table 1.⁷ Generally, we find $f_e \sim 70\%$ at a cutoff of $M^* + 0.5$ and $f_e \sim 60\%$ when including fainter members. The latter value is comparable to the fraction of passive galaxies in SG1120 with $[O II] \lambda 3727$ emission $< 5 \text{ \AA}$ ($\sim 61\% \pm 8\%$; Gonzalez et al. 2005).

4.1. f_e for Clusters

Table 2 lists f_e for galaxy clusters at a similar z as that of SG1120. Independent of magnitude cutoff, clusters at these redshifts have early-type fractions of $\sim 60\%$ (within $\sim 500 h_{65}^{-1}$

⁶ S. J. K., A. H. G., C. A. S., K.-V. H. T., and D. Z.

⁷ While mass selection is preferable to luminosity selection (e.g., Holden et al. 2006, 2007), we opt for luminosity selection in this instance to facilitate comparison with existing samples. We note however that for a stellar-mass-limited sample we obtain high f_e values comparable to cluster values from Holden et al. (2006, 2007).

TABLE 1
EARLY-TYPE FRACTIONS IN SG1120 (%)

Classification	$M^* + 0.5$	$M^* + 1$	$M^* + 1.4$	$M^* + 1.5$	$M^* + 1.75$
Visual	73 ± 4	60 ± 5	61 ± 6	61 ± 6	60 ± 6
GIM2D	66 ± 4	57 ± 4	59 ± 4	60 ± 4	58 ± 4

NOTES.—Listing for the supergroup the f_e in percentages for both the visual and automated GIM2D classification; f_e is determined using multiple magnitude cutoffs because, e.g., Simard et al. (2008) and Poggianti et al. (2006) use $M^* + 1.4$ in their sample. The error for the visual results is the standard deviation from the mean value of the visual classification from the five classifiers.

kpc; see Lubin et al. 2002 and references therein; see also van Dokkum et al. 2001; Holden et al. 2004).

We expect SG1120 to evolve into a cluster that is similar in mass to Coma. We find that Coma and SG1120 have comparable early-type fractions when similar magnitude limits are used: Holden et al. (2006) measure $f_e \sim 78\% \pm 4\%$ for luminosity-selected galaxies ($M^* + 0.5$).

4.2. f_e for Groups and the Field at $0.3 < z < 0.55$

Table 2 also lists early-type fractions for galaxy groups in the same redshift range. The first two entries in the group section refer to X-ray selected groups, and the remaining entries to kinematically selected groups. Jeltema et al. (2007) provide data for four X-ray-luminous groups. Mulchaey et al. (2006) provide two additional X-ray-luminous groups. Wilman et al. (2005) report the fraction of passive galaxies, as defined by $[\text{O II}]\lambda 3727$, within $1 h_{75}^{-1}$ Mpc of the centers of kinematically selected groups; we assume that the passive fraction corresponds to f_e , as is the case for SG1120.

The scatter in f_e is large among the galaxy group studies, but the mean early-type fraction is distinctly higher than that of the field. The field f_e is $19^{+6}_{-5}\%$ at $0.2 \leq z \leq 0.6$ (Jeltema et al. 2007), comparable to that of the passive fraction in the field ($\sim 25\%$ for $0.2 \leq z \leq 0.6$; Wilman et al. 2005).

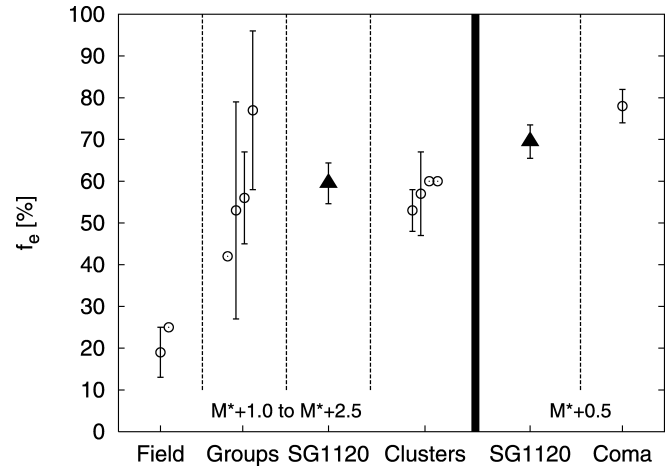


FIG. 2.—The early-type fractions as described in the text for the different environments, which are separated by dashed vertical lines. SG1120 is shown as a filled triangle and literature values as circles. SG1120 values are derived from the mean of the visual and GIM2D morphologies. The solid vertical line separates the galaxy groups and clusters at $0.3 < z \leq 0.55$ evaluated with magnitude cutoffs ranging from $M^* + 1.0$ to $M^* + 2.5$ (left panel), from a comparison to Coma ($M^* + 0.5$; right panel).

4.3. S0-to-E Ratio

The ratio of S0 to elliptical galaxies in clusters is on average 0.5 at these redshifts (Dressler et al. 1997; Desai et al. 2007). However, no measurement of the S0/E ratio has been measured for the field or for galaxy groups at intermediate redshifts. Using the visual classifications for all confirmed members in SG1120, we measure the S0/E ratio to also be 0.5, similar to clusters at the same redshift.

5. RESULTS AND DISCUSSION

Figure 2 presents f_e as a function of environment. On the left side, the values for the field, groups, and clusters for the

TABLE 2
EARLY-TYPE FRACTIONS OF GROUPS AND CLUSTERS

Source (1)	f_e (%) (2)	z (3)	Cut ($M^* +$) (4)	σ (km s^{-1}) (5)	No. (6)	Method (7)
Clusters						
Simard et al. 2008	53 ± 5	0.3–0.55	1.4	681–1080	4	GIM2D
Dressler et al. 1997	57 ± 10	0.3–0.55	2.5	n.s.	10	Visual
Desai et al. 2007 ^{a,b}	~ 60	~ 0.4	1.5	> 600	12	Visual
Lubin et al. 2002 ^b	~ 60	~ 0.4	1.5	n.s.	11	Visual
Groups						
Jeltema et al. 2007 ^c	77 ± 19	0.3–0.50	1.4	211–417	4	Visual
Mulchaey et al. 2006	53 ± 26	0.3–0.50	1.0	245–632	2	Visual
Simard et al. 2008	56 ± 11	0.3–0.55	1.4	165–540	7	GIM2D
Wilman et al. 2005	42	0.3–0.55	1.75	100–800	26	[O II]

NOTES.—The f_e of clusters and groups from in the literature. Col. (4) shows the magnitude cutoffs that were used to derive f_e . The range in velocity dispersion for the systems are given in Col. (5); if not specified in the literature, we use the “n.s.” space holder. Col. (6) contains the number of clusters/groups studied by each reference. The classification method (GIM2D, visual, or [O II] $\lambda 3727$ emission) is noted in Col. (7).

^a The galaxy cluster sample in this study overlaps with the sample in Simard et al. (2008).

^b The galaxy clusters studied in these references partially overlap with the systems of Dressler et al. (1997).

^c Here we recomputed the f_e values from the provided galaxy table for different magnitude cutoffs and found that f_e is constant over the range between $M^* + 0.5$ and $M^* + 2.5$. We therefore show only one value.

magnitude cutoffs ranging from $M^* + 1.0$ to $M^* + 2.5$ are shown. Comparing the full samples is reasonable because we found that f_e is nearly independent of the exact limit for cutoffs in this magnitude range. SG1120's early-type fraction is the mean of the visual and quantitative GIM2D classification, and its mean error is from Table 1. The right side of Figure 2 shows f_e for SG1120 and Coma using the same magnitude limit ($M^* + 0.5$).

The early-type fraction in the field is low and comparable to that measured in the local universe (e.g., Tran et al. 2001). As shown in Figure 2, f_e for galaxy clusters at the redshift range of SG1120 is $\sim 60\%$ on average (Dressler et al. 1997; van Dokkum et al. 2001; Lubin et al. 2002; Holden et al. 2004; Desai et al. 2007; Simard et al. 2008) and thus similar to the f_e measured for SG1120. In addition, SG1120's S0/E ratio is the same as that observed in galaxy clusters at the redshift of SG1120.

The early-type fraction in the galaxy groups has a larger range (Mulchaey et al. 2006; Jeltema et al. 2007); while the mean value falls below the values of SG1120 and the galaxy clusters, this may not be the most appropriate method for characterizing groups. For example, Poggianti et al. (2006) has found that the range in passive galaxy fraction corresponds to other physical characteristics, e.g., velocity dispersions of the groups. Therefore, the group population likely contains a range of systems that include preprocessed groups such as those that make up SG1120, and less evolved galaxy groups.

The Coma cluster and SG1120 ($z \sim 0.37$) both have almost comparable early-type fractions when considering the error bars ($M^* + 0.5$). Therefore, the morphological mix in SG1120, a system made of four distinct X-ray-luminous galaxy groups that will assemble into a galaxy cluster, is similar to that of clusters in the local universe. We conclude that galaxies in SG1120 are morphologically preprocessed in the group environment and so the galaxy population as a whole does not require additional morphological evolution.

While there must be some subsequent evolution due to processes such as infall of field galaxies, mergers, and ram pressure, what we learn from this system is that the net effect of

these processes need not be large. The f_e values in SG1120 indicate that late-time infall of groups does little to change the cluster early-type fraction. Holden et al. (2006, 2007) have previously demonstrated that there is little evolution in f_e for massive cluster galaxies, which is to be expected if late-time accretion is dominated by groups like those in SG1120. If late-time accretion is instead dominated by individual galaxies rather than groups, as suggested by Berrier et al. (2008), then our results imply that the accretion and transformation rates (from local and global processes) must roughly balance to maintain a stable f_e .

Although SG1120 is only a single system, it demonstrates that the cluster environment is not required to reach high early-type fractions, and that in general infalling groups should not significantly alter cluster f_e values. In fact, we see that in these group environments mergers among even the most massive galaxies are common (Tran et al. 2008) supporting the hypothesis that mergers in the group environment are a driver of galaxy evolution.

The large scatter in f_e among galaxy groups, irrespective of whether they are X-ray or kinematically selected, suggests that obtaining a clean comparison sample of groups that will be accreted by clusters is key to any evolutionary study. Thus while the weakness of our study is having only a system, representing one possible cluster assembly scenario, it is mitigated by the knowledge gained from studying galaxies in groups that are on the verge of entering the cluster environment.

We thank the anonymous referee for a thoughtful, constructive report. We are grateful to L. Simard for support with GIM2D. This work was supported by grant HST-GO-10499. K. T. acknowledges support from the Swiss National Science Foundation (grant PP002-110576), and thanks J. Blakeslee for help during the initial ACS reduction. J. M. acknowledges funding support from NASA-06-GALEX06-0030 and Spitzer G05-AR-50443.

Facilities: HST(ACS), VLT:Antu(VIMOS, FORS2), Magellan:Clay(LDSS3), Mayall(FLAMINGOS)

REFERENCES

- Barnes, J. 1985, *MNRAS*, 215, 517
 Beers, T. C., Flynn, K., & Gebhardt, K. 1990, *AJ*, 100, 32
 Berrier, J. C., Stewart, K. R., Bullock, J. S., Purcell, C. W., Barton, E. J., & Wechsler, R. H. 2008, preprint (arXiv:0804.0426)
 Desai, V., et al. 2007, *ApJ*, 660, 1151
 Dressler, A. 1980, *ApJ*, 236, 351
 Dressler, A., et al. 1997, *ApJ*, 490, 577
 Fabricant, D., Franx, M., & van Dokkum, P. 2000, *ApJ*, 539, 577
 Fruchter, A. S., & Hook, R. N. 2002, *PASP*, 114, 144
 Gómez, P. L., et al. 2003, *ApJ*, 584, 210
 Gonzalez, A. H., Tran, K.-V. H., Conbere, M. N., & Zaritsky, D. 2005, *ApJ*, 624, L73
 Gunn, J. E., & Gott, J. R., III. 1972, *ApJ*, 176, 1
 Graham, A. W., Erwin, P., Trujillo, I., & Asensio Ramos, A. 2003, *AJ*, 125, 2951
 Helsdon, S. F., & Ponman, T. J. 2003, *MNRAS*, 339, L29
 Holden, B. P., Stanford, S. A., Eisenhardt, P., & Dickinson, M. 2004, *AJ*, 127, 2484
 Holden, B. P., et al. 2006, *ApJ*, 642, L123
 ———. 2007, *ApJ*, 670, 190
 Jeltema, T. E., Mulchaey, J. S., Lubin, L. M., & Fassnacht, C. D. 2007, *ApJ*, 658, 865
 Kodama, T., Smail, I., Nakata, F., Okamura, S., & Bower, R. G. 2001, *ApJ*, 562, L9 (erratum 591, L169 [2003])
 Krist, J. 1993, in ASP Conf. Ser. 52, *Astronomical Data Analysis Software and Systems II*, ed. R. J. Hanisch et al. (San Francisco: ASP), 536
 Larson, R. B., Tinsley, B. M., & Caldwell, C. N. 1980, *ApJ*, 237, 692
 Lewis, I., et al. 2002, *MNRAS*, 334, 673
 Lubin, L. M., Oke, J. B., & Postman, M. 2002, *AJ*, 124, 1905
 Mastropietro, C., et al. 2005, *MNRAS*, 364, 607
 Moore, B., Lake, G., Quinn, T., & Stadel, J. 1999, *MNRAS*, 304, 465
 Mulchaey, J. S., Lubin, L. M., Fassnacht, C. D., Rosati, P., & Jeltema, T. E. 2006, *ApJ*, 646, 133
 Park, C., Choi, Y.-Y., Vogeley, M. S., Gott, J. R., III, & Blanton, M. R. 2007, *ApJ*, 658, 898
 Poggianti, B. M., et al. 2006, *ApJ*, 642, 188
 Postman, M., et al. 2005, *ApJ*, 623, 721
 Simard, L., et al. 2002, *ApJS*, 142, 1
 ———. 2008, *A&A*, submitted
 Toomre, A. 1977, in *Evolution of Galaxies and Stellar Populations*, ed. B. M. Tinsley & R. B. Larsen (New Haven: Yale Univ. Obs.), 402
 Tran, K.-V. H., Moustakas, J., Gonzalez, A. H., Bai, L., Zaritsky, D., & Kautsch, S. J. 2008, *ApJ*, 683, L17
 Tran, K.-V. H., Simard, L., Zabludoff, A. I., & Mulchaey, J. S. 2001, *ApJ*, 549, 172
 van Dokkum, P. G., Stanford, S. A., Holden, B. P., Eisenhardt, P. R., Dickinson, M., & Elston, R. 2001, *ApJ*, 552, L101
 Wilman, D. J., et al. 2005, *MNRAS*, 358, 88
 Zabludoff, A. I., & Mulchaey, J. S. 1998, *ApJ*, 496, 39